International Journal of the Physical Sciences Vol. 6(3), pp. 459-475, 4 February, 2011
Available online at http://www.academicjournals.org/IJPS
DOI: 10.5897/IJPS10.682
ISSN 1992 - 1950 ©2011 Academic Journals

Full Length Research Paper

Tsunami simulation of the October 25, 2010, South Pagai Island, Sumatra earthquake

Ergin Ulutaş

Department of Geophysical Engineering, Faculty of Engineering, Kocaeli University, Kocaeli, Turkey. E-mail: ergin@kocaeli.edu.tr. Tel: +90 262 303 31 16. Fax: +90 262 303 30 03.

Accepted 17 January 2011

In this study, two kinds of tsunami numerical models based on the shallow water equations were employed to simulate the South Pagai Island, Sumatra earthquake tsunami which occurred in 25 October 2010. The models consist of generation, propagation and arrival times along affected coasts in Mentawai islands. Post event tsunami calculations were performed in order to better represent the event and identify more in detail the affected locations. The numerical models were performed by using nonlinear and dispersive long wave tsunami models (TUNAMI N2 and SWAN) with GEBCO30 and ETOPO2 bathymetry data in a coarse 2′ and 4′ basin scale grid. The simulated waves were particulary high on the South shore of the islands of Mentawai where they reached. This is in agreement with the locations indicated by the survey reports as most affected. The simulated waves were also compared with the available deep ocean pressure sensors and tide gauge records. Results of the numerical simulations except for the Padang2 tide gauge measurement are in reasonable agreement with data of observations. In this regard, numerical simulations are important for the purpose of providing mitigation measures to reduce the potential impacts and risks on local communities in the islands. Therefore, the main purpose of this study was conducted to contribute to reveal the effects of the earthquake in the region by using the tsunami simulation models considering the occurrence of tsunami in the future at the same area.

Key words: Mentawai Islands, earthquake source parameters, tsunami, tsunami simulation, bathymetry

INTRODUCTİON

The great Sumatra earthquake of 26 December 2004 with a moment magnitude of 9.3 was the second-largest instrumentally recorded earthquake in history (Stein and Okal, 2005). The associated tsunami run-up height was reported to have reached 2.5 to 11 m (Borrero et al., 2006) along the Sumatra coasts. The tsunami hit the Indian Ocean region and caused more than 283.000 deaths (Lay et al., 2005). This earthquake has renewed Indonesians awareness of the importance of tsunami simulation and early warning system studies. The needs for community education, preparedness and mitigation to face potential tsunami threats along the coastal regions in Indonesia have been highlighted since the occurrence of the earthquake. However, an earthquake which occurred in Mentawai Island on 25 October 2010 with a 7.7 magnitude lower than great Sumatra Earthquake killed 449 people (Lestariningsih, 2010). Although tragic, the number of deaths was fortunately far smaller than in the case of the 2004 great Sumatra tsunami due to the lower magnitude of the earthquake and low population density on the Mentawai Island coasts.

According to the information available on the web, the tsunami traces on the shore were examined by specialists from the ADRC (Asian Disaster Reduction

Abbreviations: ADRC, Asian Disaster Reduction Center; **CFL,** Courant-Friedrichs-Lewy; **DART,** Deep-ocean Assessment and Reporting of Tsunamis; **GEBCO,** General Bathymetric Chart of the Ocean; **GLOSS,** Global Sea Level Observing System; **IOS,** Intergovernmental Oceanographic Commission; **NOAA,** National Geophysical Data Center; **TIME,** Tsunami Inundation Modeling Exchange; **TAT,** Tsunami Assesment Tool; **USGS,** United States Geological Survey.

Figure 1. Tsunami hit area in South Pagai (http://www.allvoices.com/contributed-ews/7166912).

Figure 2. Tsunami hit area in Muntei Baru Baru (http://www.dailymail.co.uk/news/article-1324162).

Center) and Sikakap and Padang Coordination team (Koresawa, 2010; Lestariningsih, 2010). The conducted field surveys immediately after the earthquake have not been reported yet on the available peer-reviewed papers. This earthquake triggered a tsunami that pounded remote island villages in Mentawai Islands of Indonessia (Figures 1, 2, 3, 4, 5 and 6). Unfortunatelly, part of Indonesia's tsunami warning system failed because two buoys off the Mentawai islands had been vandalized and were not working. According to the officials there were problems with the warning system that was designed to alert local people for tsunami danger (BBC, 2010).

Figure 3. Tsunami-hit area in South Pagai (http://www.allvoices.com/contributed-news/7166912).

Figure 4. Tsunami-hit area in Bulasat (http://mentawaiblog.blogspot.com/2010/10/mentawai-earthquake-and-tsunami-photos.html).

The October 25, 2010 earthquake struck Mentawai Island District in West Sumatra Province and tsunami affected a large number of villages in sub-districts of South Pagai, North Pagai, Sikakap, South Sipora (Tables 1 and 2). According to the USGS (United States Geological Survey), the epicenter was located on 3.61° South Latitude and 100.117° East Longtitude at a depth of 20.6 km. The distance from the epicenter is 78 km to South

Figure 5. Tsunami-hit area in Bulasat (http://mentawaiblog.blogspot.com/2010/10/mentawai-earthquake-and-tsunami-photos.html).

Figure 6. Tsunami-hit area in Tumarei (http://mentawaiblog.blogspot.com/2010/10/mentawai-earthquake-and-tsunami-photos.html).

Table 1. The affected areas are 15 villages which lie in 4 sub-districts (North Pagai, South Pagai, Sikakap, South Sipora) (Lestariningsih, 2010).

Type	Community buildings	Government buildings	Schools	Religious worship	Public facilities
Heavy damage	516	6	6	8	7 Bridges and 8 km roads,1 boat, 2 resorts
Minor damage	204				

Table 2. The number of deaths and injures reported by Caritas Indonessia (Lestariningsih, 2010).

Death	Severe Injures	Minor Injures
449	27	142

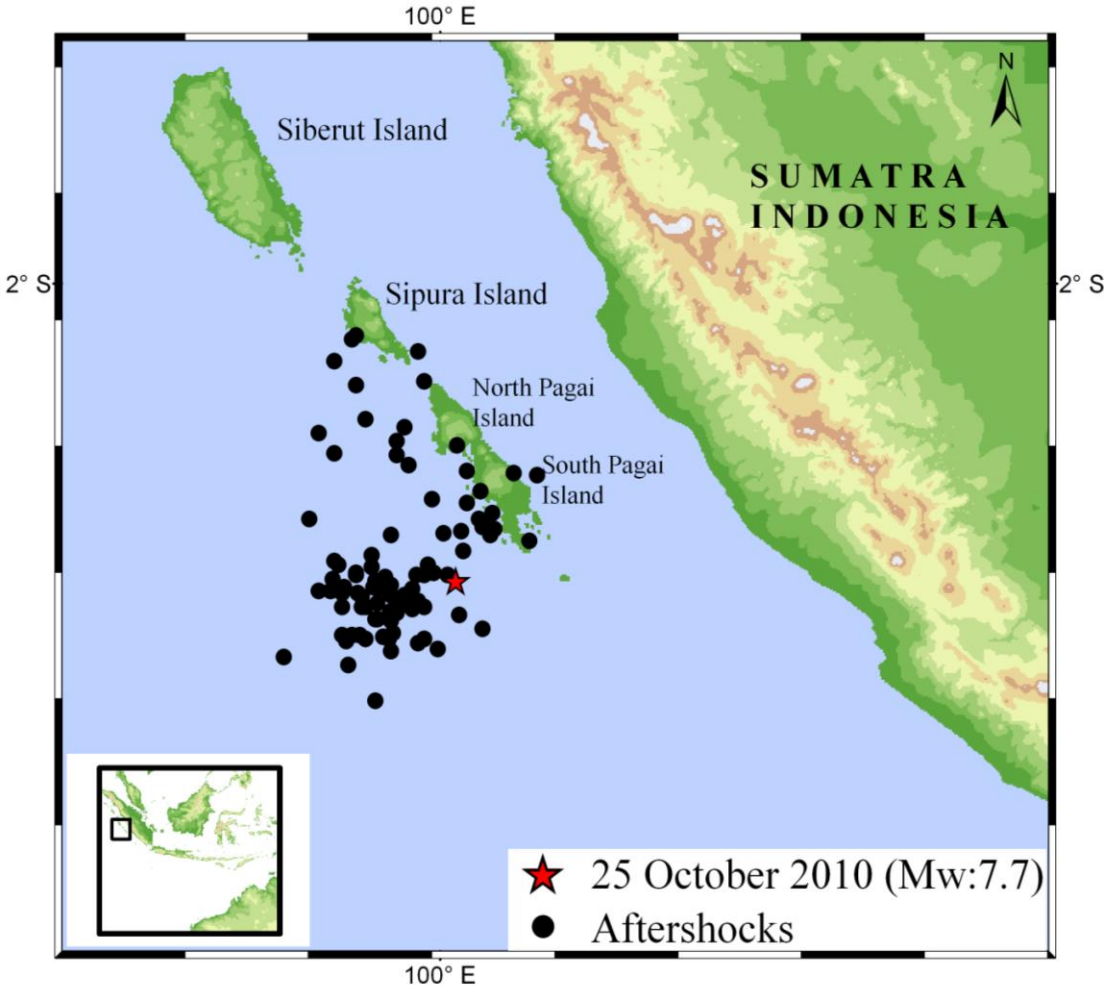

Figure 7. The epicenter of the main shock and numerous aftershocks within a week (earthquakes are reported by USGS).

West of South Pagai, Mentawai Island, to 240 km West of Bengkulu, Sumatra, Indonesia, to 280 km South of Padang, Sumatra, Indonesia, and to 795 km West North West of Jakarta, Java, Indonesia. Figure 7 shows the epicenter of the main shock and the aftershocks within a week. The main shock and aftershocks occurred along a fault line from the South Pagai Island to the Siberut Island where the Indo-Australian plate subducting Sunda and Burma sub-plates. The Australian plate subducts Sunda plate at a velocity of roughly 60 mm/year (Wang and Liu, 2006). There is a potential for tsunamis in the subduction zone, if such an earthquake causes rapid deformation of the sea floor. In the wake of the 2010 Sauth Pagai Island, Sumatra earthquake, it is important to assess the tsunami hazard which may threaten the Mentawai Island coasts.

TSUNAMI GENERATION, MODELLING AND ANALYSIS

Tsunami is generated by a series of waves when a large volume of water body, such as an ocean, is rapidly displaced. The sources of displacement are associated with the catastrophic events such as earthquakes, landslides, volcanic eruptions and collision of astroids.

This study focused on the tsunamis related to tectonic earthquakes. Tectonic earthquakes are particular kinds of earthquakes that are associated with the earth's crustal deformation. When these earthquakes occur beneath the sea, the water above the deformed area is displaced from its equilibrium position. Then, waves are formed as the displaced water mass, which acts under the influence of gravity, attempts to regain its equilibrium. The final amplitude of a tsunami wave at coasts is a combination of the amplitude of the tsunami on the high seas, and of the response of the coastal area to the wave, the latter itself is a combination of the so-called 'run-up' expressing the increase in wave amplitude upon schoaling (Okal, 1988).

Until recently, it was common to choose a tsunami-like water surface as the initial condition for mathematical solution of the long-wave equations (Mader, 1988; Titov and Synolakis, 1998; Titov and Gonzales, 1997; Shuto et al., 1990; Yalçıner et al., 2000, 2002; Pelinovsky et al., 2001; Zahibo et al., 2003; Yalçıner et al., 1995; Yalçıner and Pelinovsky, 2007; Franchello, 2008; Yolsal et al., 2008, Annunziato et al., 2009).

The long wave (shallow water) equations describe the evolution of incompressible flow, neglecting density change along the depth. Shallow water wave equations are applicable to cases where the horizontal scale of the flow is much bigger than the depth of the fluid. Therefore, tsunami waves can be described by shallow water models (Liu et al., 2009). In this study, TUNAMI N2 and SWAN models were used to simulate the tsunami wave propagation.

The simulation models solve the non-linear long wave (shallow water) equations of the fluid flow, using an explicit in time finite difference scheme (Mader, 1988). The set of equations to be solved are:

$$u_t + \frac{1}{\cos(\varphi)} + uu_x + vu_y + \frac{g}{\cos(\varphi)} + \eta_x = fv - \frac{g|U|u}{C^2(D+\eta)} \quad (1)$$

$$v_t + \frac{1}{\cos(\varphi)} + uv_x + vv_y + g\eta_y = -fu - \frac{g|U|v}{C^2(D+\eta)} \quad (2)$$

$$u_t + \frac{1}{\cos(\varphi)}\{[(\eta+D)u]_x + [(\eta+D)v\cos(\varphi)]_y\} = 0 \quad (3)$$

where φ is the latitude, u and v are the x and y components of the velocity U, g is the gravitational acceleration, t is the time, η is the wave height above the mean water level, f is the Coriolis parameter, C is the coefficient for bottom stress, D is the depth, and indexes refer to partial derivatives.

In this study, the approximation of shallow water equations was performed in geographical coordinates and was adopted to simulate tsunami propagations with an initial displacement of the ocean bottom deformation due to faulting.

SWAN code was initially proposed by Mader (1988). Annunziato (2007) adapted the model to Early Warning Systems by including some tools in order to explore and quickly retrieve tsunami arrival times and run-up heights. The model TUNAMI N2 was originally developed in Disaster Control Research Center in Tohoku University (Japan) through the TIME (Tsunami Inundation Modeling Exchange) program (Goto et al., 1997). TUNAMI N2 is one of the key tools to study propagation and coastal amplification of tsunamis in relation to different initial conditions (Goto and Ogawa, 1982; Imamura and Shuto, 1989; Goto et al., 1997 Shuto and Goto, 1988; Shuto et al., 1990). TUNAMI N2 code was implemented to simulate tsunami propagation and run-up in Pacific, Atlantic and Indian Oceans, with zoom-in at particular areas of Japanese, Caribbean, Russian, and Mediterranean seas (Yalçıner et al., 2000, 2001, 2002, 2004; Zahibo et al., 2003; Tinti et al., 2006).

Tsunami source model

The choice of the tsunami source is usually a complicated problem because it requires a good knowledge of the earthquake parameters such as epicenter, depth, fault length, fault width, slip distribution and rupture mechanism. The simulations for the tsunamis could be generated by the coseismic displacement of the sea floor. Thus, the initial condition for the expected tsunami in the region has to be taken to coincide with the vertical coseismic displacement of the sea bottom induced by the earthquake. The initial conditions are one of the major factors that affect the resulting run up amplitudes along the shoreline. Different approaches can be used to calculate the initial conditions from the motion of the fault. In this study, the initial tsunami surface is applied the same displacement as the vertical deformation of the ocean bottom due to the earthquake. The ocean bottom displacement, assumed to be responsible for the initial water surface deformation giving rise to the tsunami, was computed using the dislocation algoritm provided by Okada (1985). This algoritm calculates the distribution of coseismic uplift and subsidence by using the epicenter of earthquake, strike, dip, rake of the fault and amount of average displacement on the fault. And also a rectangular fault model was assumed for the dislocation area and it was obtained by available empirical relations. The relations between fault rupture length-magnitude and fault rupture width-magnitude were used as in the following equations (Wells and Coppersmith, 1994):

$$\mathrm{LogL} = -2.42 + 0.58\mathrm{M} \quad (4)$$

and

$$\mathrm{LogW} = -1.61 + 0.41\mathrm{M} \quad (5)$$

where M is the moment magnitude, L is the subsurface rupture lenght (km) and W is the downdip rupture width (km).

The earthquake parameters and fault mechanism solutions which were available after the earthquake are given respectively in Table 3. The mechanism solutions show an almost reverse fault, on a plane striking roughly parallel to the Sunda Trench axis, with seismic moment of 6.66×10^{27} dyn cm (USGS, 2010).

Bathymetry data, DART and tide gauge stations

The bathymetry data plays an important role in the outcome of tsunami simulations. For a tsunami wave in deep water, the propagation velocity is approximately proportional to the square root of the water depth,

$$\mathrm{c} = \sqrt{\mathrm{gh}} \quad (6)$$

where c is the wave propagation velocity, g is the gravity acceleration, and h is the ocean depth.

For instance, the tsunami wave travels at a velocity of 796 km/h (approximately the speed of a jet airplane) at 5000 m water depth. The velocity drops to 252 km/h for a water depth of 500 m. The velocity of wave propagation drops dramatically, when shallow continental shelf regions are encountered. Thus, a good regional bathymetric model is required for accurately modeling tsunami arrival times (Gutscher et al., 2006). Here, two bathymetric data sets with different resolutions were used to compare the results and to underline the effects of bathymetric data on tsunami

Table 3. Earthquake parameters of tsunami source for the 25 October 2010 South Pagai Island, Sumatra earthquake.

Earthquake magnitude(M_w)	Latitude	Longtitude	*Fault lenght(km)	*Fault width(km)	**Strike	**Dip	**Rake	Slip
7.7	3.484^0S	100.114^0E	111.17	35.23	319	7	98	2.56

*It has been calculated by using the Wells and Coppersmith(1994)empirical ralationssip for reverse faults.** Available immediatelly after the earthquake from U.S. Geological website (http://earthquake.usgs.gov/earthquakes/eqinthenews/2010/usa00043nx/neic_a00043nx_gcmt.php.

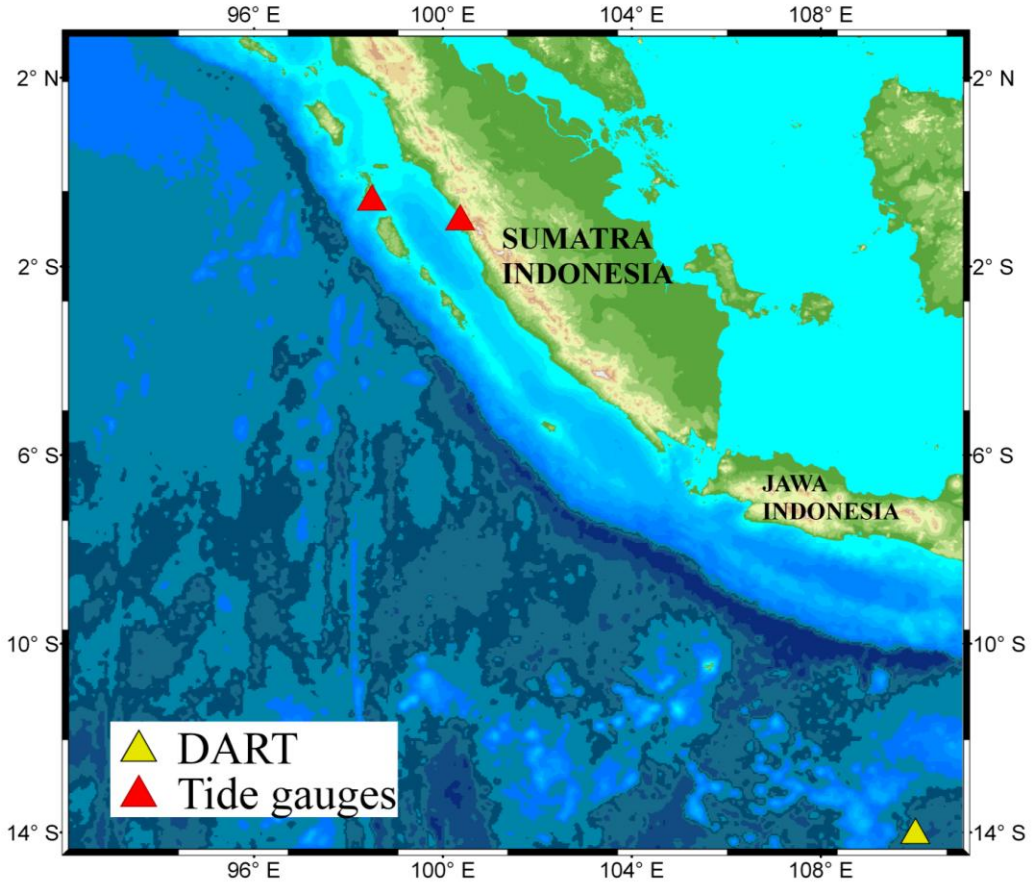

Figure 8. Computation area (A) for Numerical models with ETOPO2 bathymetry.

simulation. One of them is ETOPO2 produced by the NOAA (National Geophysical Data Center) with the 2 min grid size (ETOPO2, NGDC/NOAA). The ETOPO2 is a combination of satellite altimetry observations, shipboard echo-sounding measurements, data from the Digital Bathymetric Data Base Variable Resolution and data from the GLOBE project which has a global digital elevation model. The other is GEBCO (General Bathymetric Chart of the Ocean)(GEBCO30, IHO/UNESCO). The computation of the area of tsunami area of tsunami computation with ETOPO2 and GEBCO30 were displayed in Figures 8 and 9 respectively.

One deep ocean pressure sensor named DART (Deep-ocean Assessment and Reporting of Tsunamis) and two tide gauge stations were used as the comparison points of tsunami simulation. Figure 8 also shows the distribution of DART and tide gauges in the computational area. In Figure 8, the DART station represented by the yellow triangle is operated by the Australian Bureau of Meteorology and the tide gauges represented by the red triangles are operated by the University of Hawaii Sea Level Center (USA) and GeoForschungsZentrum (Germany).

The one deep ocean pressure sensor named DART (Deep-ocean Assessment and Reporting of Tsunamis) and two tide gage stations were used as the comparison points of tsunami simulation. Figure 8 also shows the distribution of DART and tide gauges in the computational area. In Figure 8, the DART station represented by yellow triangle is operated by Australian Bureau of Meteorology and

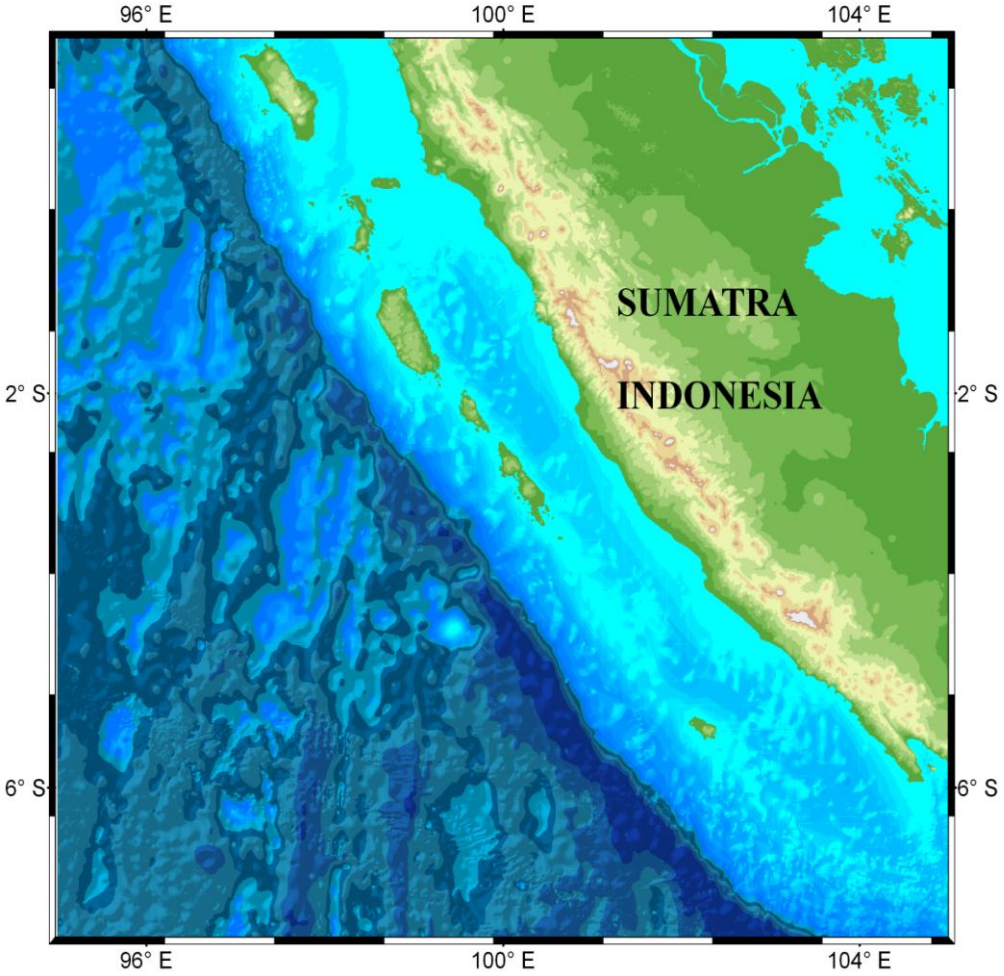

Figure 9. Computation area (B) for Numerical models with GEBCO30 bathymetry .

the tide gauges represented by red triangles are operated by University of Hawaii Sea Level Center (USA) and GeoForschungsZentrum (Germany).

Computational analysis, comparisons and results

Numerical simulations of tsunami waves generated by an earhquake which occurred offshore Mentawai Islands as thrust-faulting along the Australian and Sunda plates have been performed. The computation area was set in two parts as A and B. The first area one covers 2.0 to 8.0°S and 95.0 to 105.0°E, and the second one covers 2.0 to 15.0°S and 92.0 to 111.0°E. At the computation area A, 4′ grid is used to calculate tsunami height in the location where the DART installed. At the computation area B, 2′ and 0.5′ grid was used with ETOPO2 and GEBCO30 bathymetry data sets.

The vertical crustal dislocation caused by uniform faulting was computed as the initial condition for tsunami. For this computation, Okada's (1985) algoritm was used as previously mentioned. Figure 10 shows the vertical seafloor displacement and Figure 11 illustrates the cross-section of the vertical seafloor dislocation along line AB from Okada's (1985) algoritm with source parameters determined by USGS (2010). The displacement beneath the seafloor, with a maximum of 55 cm, is responsible for tsunami generation. The maps of maximum tsunami amplitude (h_{max}) maps from each bathymetry and each model are shown in Figures 12, 13,14,15,16 and 17. The time step of 0.5 s is set to satisfy the CFL (Courant-Friedrichs-Lewy) stability condition. The total calculation time was set to three hours for the computation area A, and the total calculation time was set to one hour for the computation area B. To obtain the maximum heights on the locations and tsunami arrival times, Tsunami Assesment Tool (TAT) software was used, which was originally developed by Annunziato (2007). The system allows a direct comparison with the available sea level measurements downloaded from IOC/GLOSS (Intergovernmental Oceanographic Commission / Global Sea Level Observing System) and NOAA web sources (Annunziato, 2010).

According to the assumed shape of initial sea surface dislocation, a wave with leading trough propagates through the South and North Pagai, while a wave with leading crest propagates to offshore. In these simulations, tsunami immediately hit the Southern coasts of Mentawai Islands (South and North Pagai) with the wave height exceeding 3.1 and 3.8 m due to the SWAN and TUNAMI N2 models with GEBCO30 bathymetry respectively (Figure 12 and 17). The figures show that most of the tsunami's energy travels perpendicular to the strike of the fault segment which is evident from the theory of directivity (Heidarzadeh et al., 2008). The

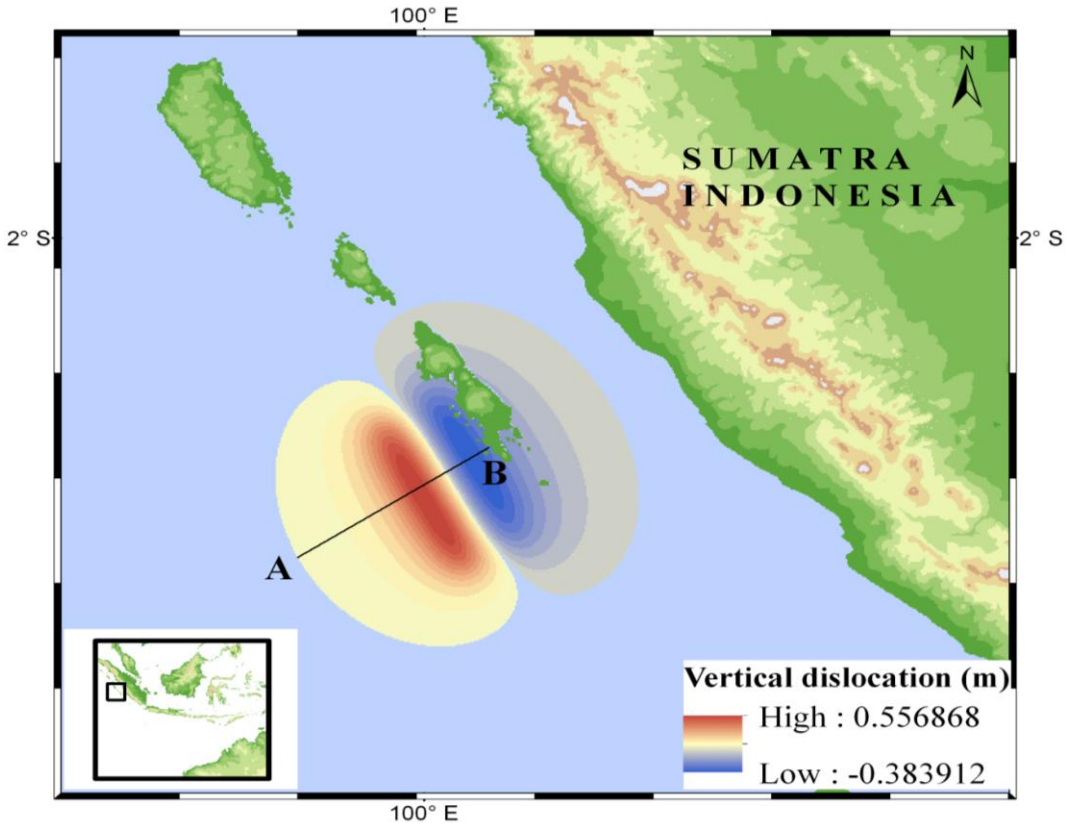

Figure 10. Vertical displacement of the seafloor.

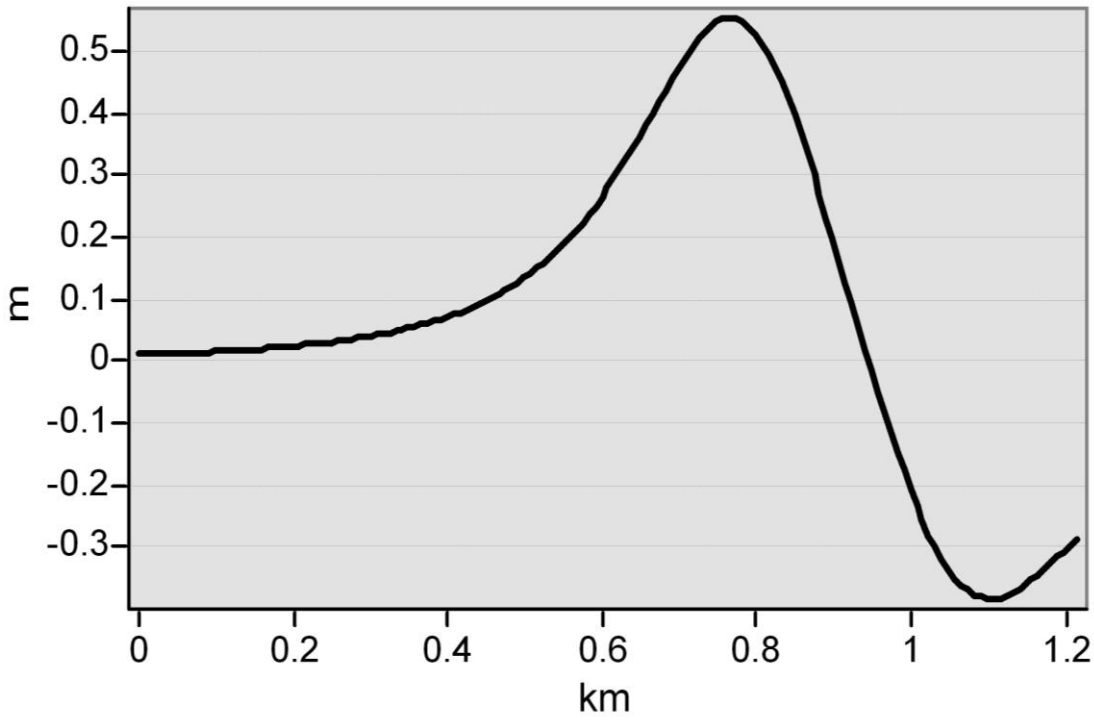

Figure 11. A cross-section of the vertical seafloor displacement along line AB.

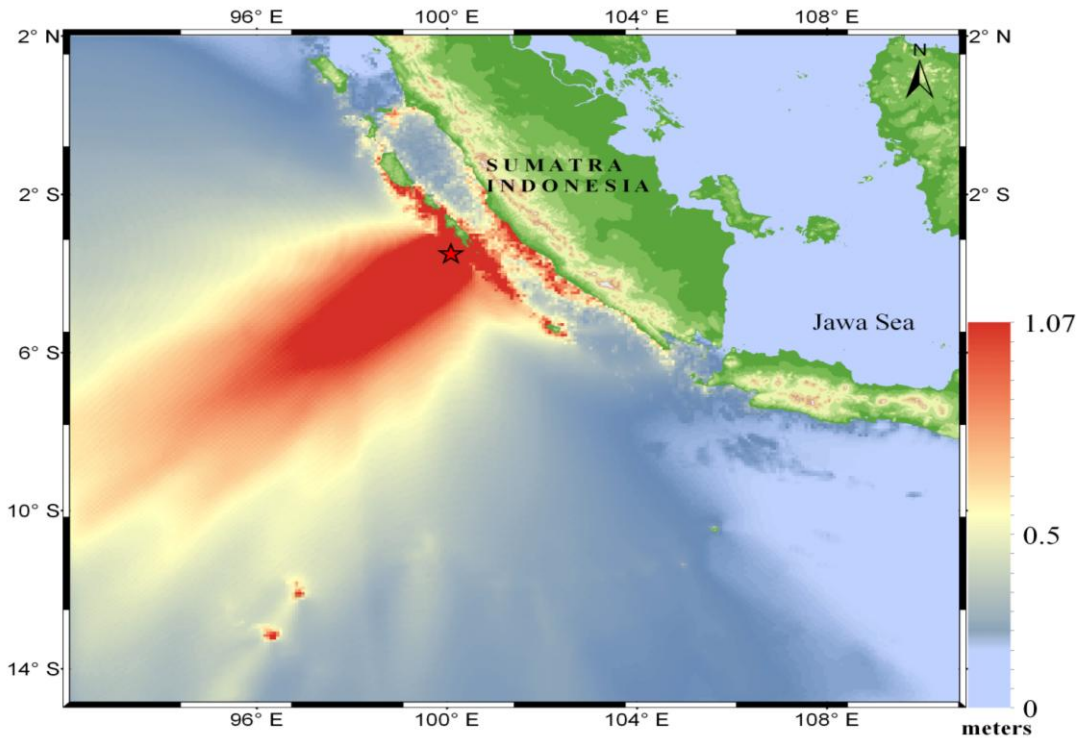

Figure 12. Maximum tsunami height due to the ETOPO2 bathymetry with a grid spacing of 4′ (SWAN Model).

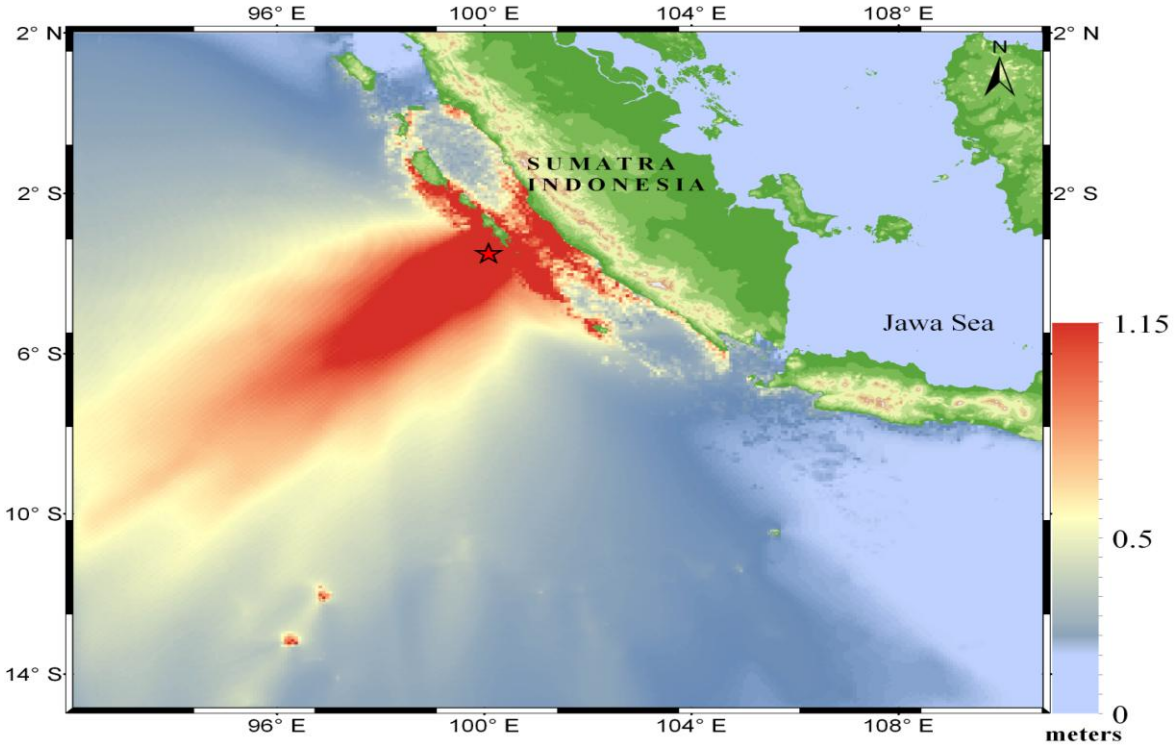

Figure 13. Maximum tsunami height due to the GEBCO30 bathymetry with a grid spacing of 4′ (SWAN Model).

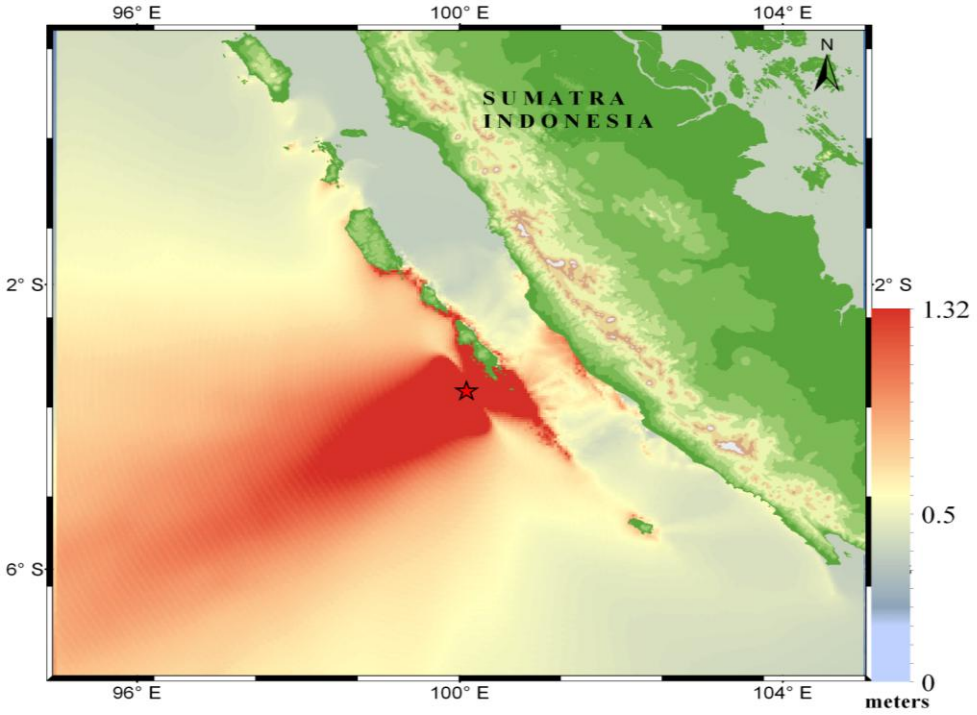

Figure 14. Maximum tsunami height due to the ETOPO2 bathymetry with a grid spacing of 2′ (SWAN Model).

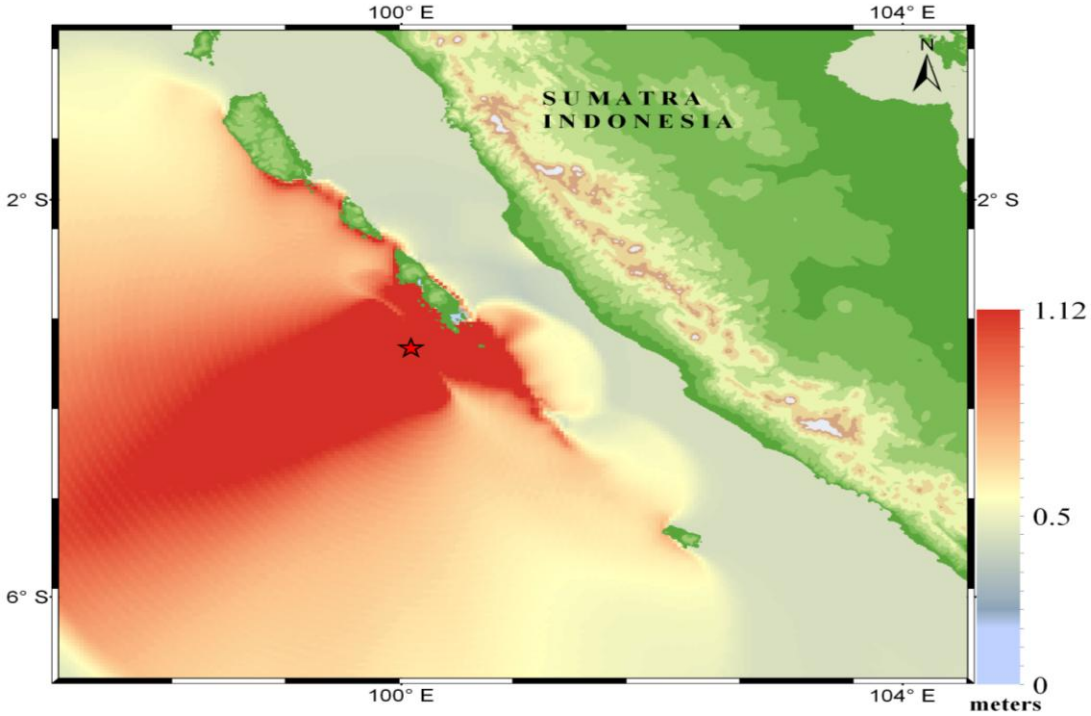

Figure 15. Maximum tsunami height due to the ETOPO2 bathymetry with a grid spacing of 2′ (TUNAMI N2 Model).

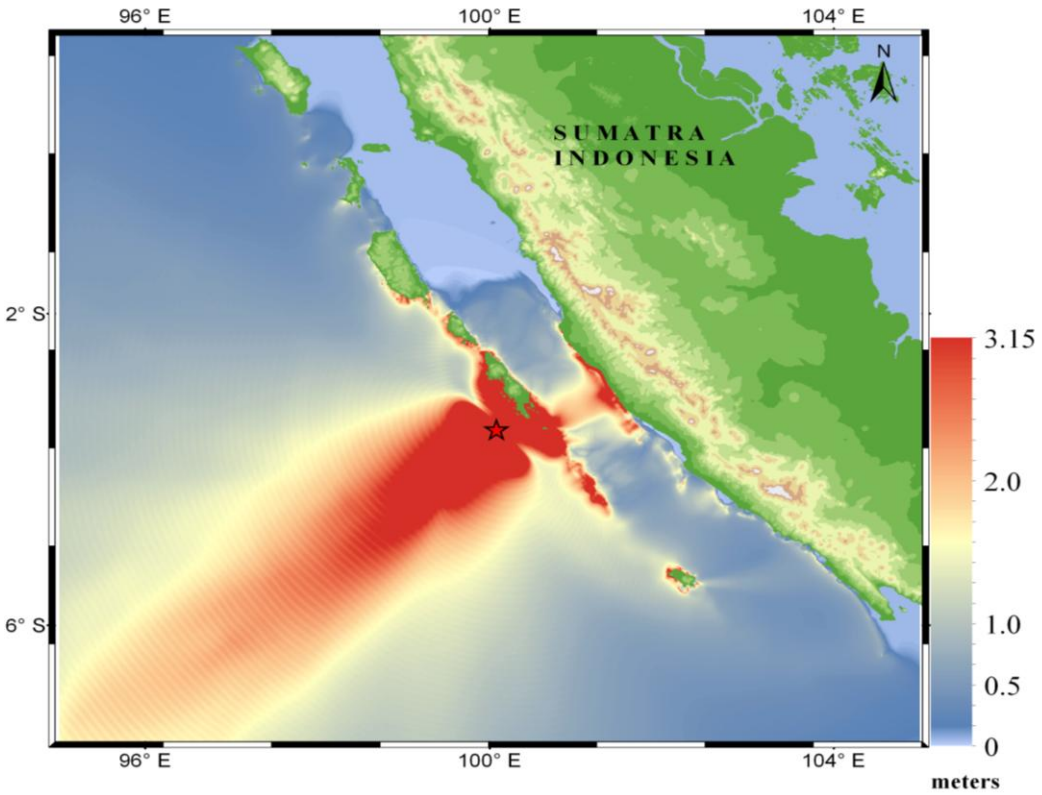

Figure 16. Maximum tsunami height due to the GEBCO30 bathymetry with a grid spacing of 0.5′ (SWAN Model).

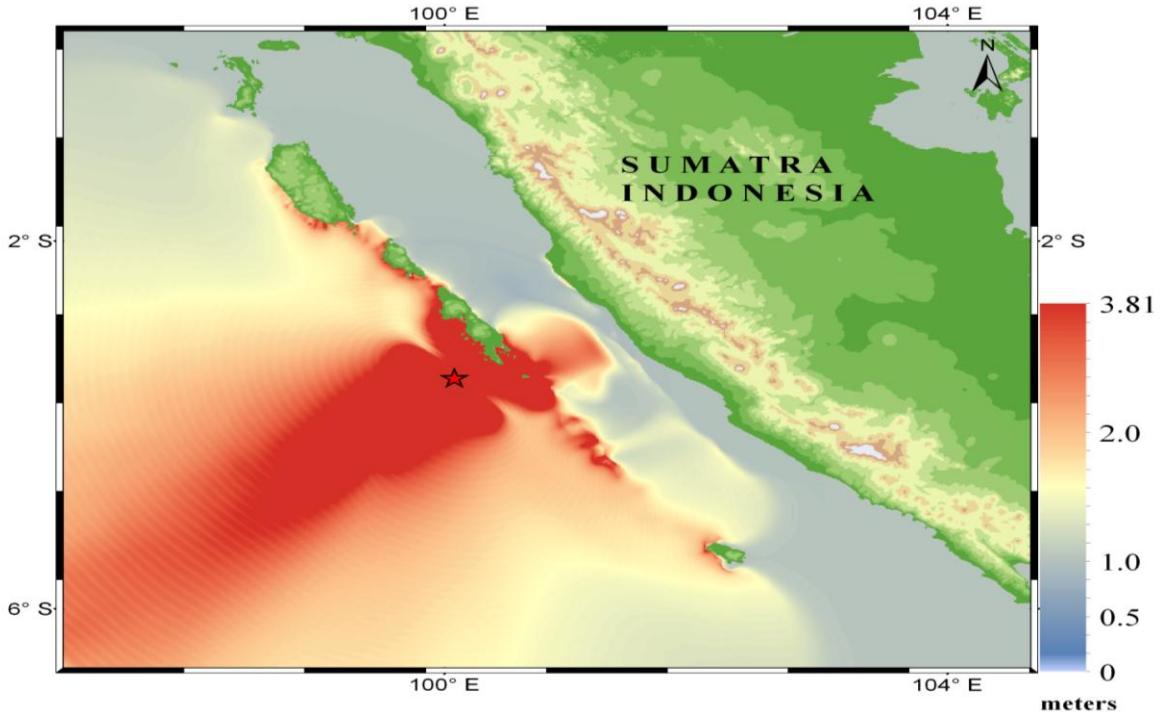

Figure 17. Maximum tsunami height due to the GEBCO30 bathymetry with a grid spacing of 0.5′ (TUNAMI N2 Model).

Table 4. Heights of maxımum tsunami waves.

Location (village or dorp)	LAT	LONG	[1]Maximum height	[2]Maximum height	[3]Maximum height	[4]Maximum height
Tiop	-3.21	100.36	2.9	3.6	1.1	1.1
Bulasat	-3.07	100.28	2.2	2.9	1	0.9
Beleratsok	-2.94	100.20	1.4	1.5	0.8	0.8
Buriai	-3.10	100.45	1.0	1.0	0.4	0.7
Silaoinan	-2.78	100.14	0.5	0.5	0.4	0.5
Kaliet	-2.36	99.80	0.4	0.4	0.2	0.2
Katiet	-2.38	99.84	0.4	0.4	0.2	0.2
Maileppet	-2.24	99.61	0.4	0.4	0.2	0.2
Beriolou	-2.33	99.72	0.4	0.3	0.2	0.1
Simagandjo	-2.59	100.06	0.2	0.1	0.1	0.1

[1]Maximum heights, modeled by SWAN model due to the GEBCO 30 bathymety with a 0.5′ grid calculation space. [2]Maximum heights, modeled by TUNAMI N2 model due to the GEBCO 30 bathymety with a 0.5′ grid calculation space. [3]Maximum heights, modeled by SWAN model due to the ETOPO2 bathymety with a 2′ grid calculation space. [4]Maximum heights, modeled by SWAN model due to the ETOPO2 bathymety with a 4′ grid calculation space.

Table 5. Arrival times of maximum tsunami heights.

Location (village or dorp)	LAT	LONG	[1]Arrival time	[2]Arrival time	[3]Arrival time	[4]Arrival time
Beleratsok	-2.94	100.20	14:58:08	14:58:54	14:57:23	14:53:45
Beriolou	-2.33	99.72	15:27:25	15:08:00	15:29:41	14:56:47
Bulasat	-3.07	100.28	14:58:54	15:03:27	14:51:28	14:49:12
Buriai	-3.10	100.45	15:23:01	15:16:57	15:41:50	16:01:14
Kaliet	-2.36	99.80	15:05:44	15:06:29	15:29:41	16:03:31
Katiet	-2.38	99.84	15:05:44	15:06:29	15:29:41	16:03:31
Maileppet	-2.24	99.61	15:19:14	15:05:44	15:23:46	14:58:54
Silaoinan	-2.78	100.14	15:16:57	15:16:57	14:57:23	14:52:14
Simagandjo	-2.59	100.06	15:30:27	15:16:57	15:01:10	15:01:56
Tiop	-3.21	100.36	14:58:08	15:00:25	14:52:59	14:57:23

[1]Arrival times, modeled by SWAN model due to the GEBCO 30 bathymety with a 0.5′ grid calculation space. [2]Arrival times, modeled by TUNAMI N2 model due to the GEBCO 30 bathymety with a 0.5′ grid calculation space. [3]Arrival times, modeled by SWAN model due to the ETOPO2bathymety with a 2′ grid calculation space. [4]Arrival times, modeled by SWAN model due to the ETOPO2bathymety with a 4′ grid calculation space.

selected locations affected by tsunami in South and North Pagai Island with maximum heights and arrival times of maximum heights were displayed in Tables 4 and 5 respectively. It can be seen that the maximum heights and arrival times were different at the same locations. The differences between the maximum heights andarrival times were due to the use of various computational grid points and bathymetry resolution. In order to compare the simulation results with the survey results, available preliminary reports on web after the tsunami were compiled (Table 6). However, the effects of the earthquake, tsunami in Mentawai Islands, including wave amplitudes and extent of inundation, have not been well documented yet on the available peer-reviewed papers. It is only possible to compare one village named Bulasat with the simulation results. According to the TUNAMI N2 simulation with GEBCO30 bathymetry, It can be seen that Bulasat village and nearest village to Bulasat named Tiop were mostly affected from tsunami with about 3 m height. However, the observed heights for the Bulasat village were between 6.4 and 9.3 m. This discrepancy should be due to the local bathymetric features. Nevertheles, the simulated maximum wave heights were calculated for the same places that were mostly affected from tsunami. Detailed and more local calculations are needed in order to correctly analyze the local behaviour and estimate the height in specified locations. The maximum heights were also calculated about 1.1 in the villages due to the ETOPO2 bathymetry with and 2′and 4′ grid calculation space. It is much more less than the 3.0 m because calculation space is larger than 0.5′ and bathymetry resolution is lower than GEBCO30. The calculations performed with 2′ and 4′ grid size was not able to identify the tsunami heights in some villages but a very high enery above that island was reported (Table 6).

Numerical simulation results were also compared with available deep ocean pressure sensors (DART) and tidal gauge

Table 6. Field survey results of tsunami stricken areas in the Mentawai Islands (Koresawa, 2010).

Sub-district	Village	Dorp	Observed tsunami height range (m)	Population	Casualty
North Pagai	Silabu	Tumalei	4.0-6.0	199	5
		Macaronis resort	2.9-5.4	20 visitors	1
	Metomonga	Sabeu Guggung	4.3-7.0	258	121
		Muntei	4.6-7.8	314	114
		Muntei coast	3.9-8.8		
		Purorougat	5.5	235	72
		Lakau	2.5		0
Sauth Pagai	Bulasat	Asahan	6.4-9.3		0
		Maonai	6.3-6.9	139	35

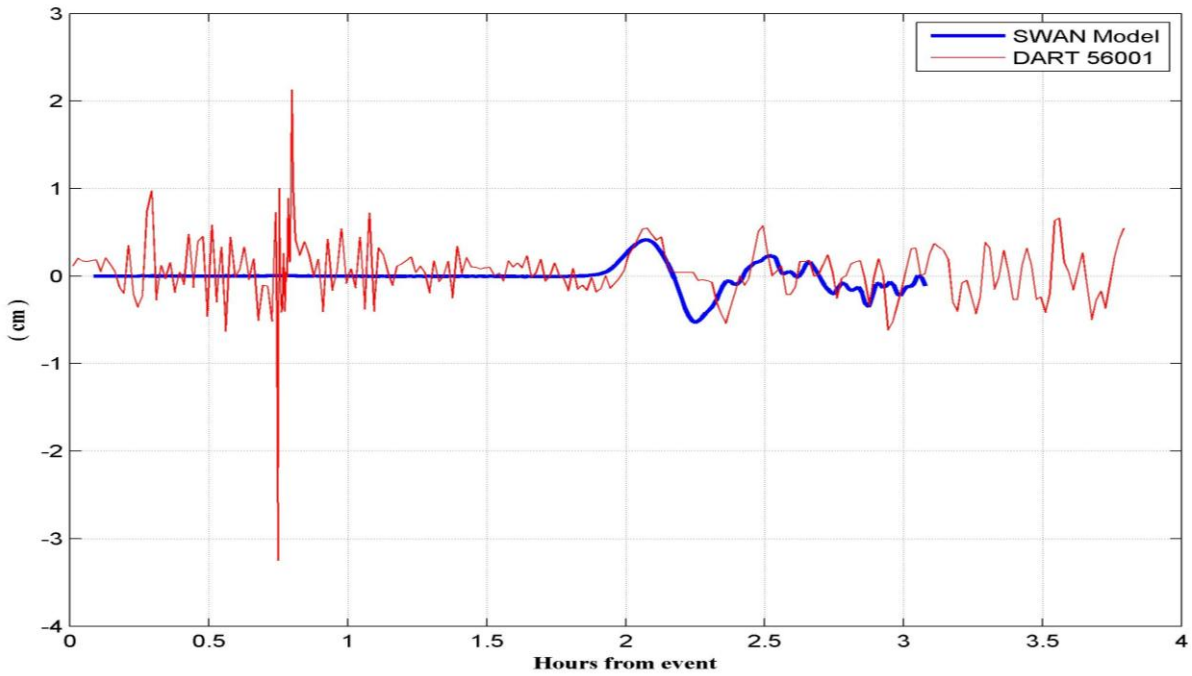

Figure 18. Comparison with DART (56001) buoy measurement based on SWAN model with a ETOPO2 bathymetry.

measurements. Observations of sea level in the deep ocean were available for this event from a DART buoy (56001) at (-13.9610S, 110.00400E), tide gauges (Tanahbalah) at (-0.53260S -98.4977 and (Padang2) at (-0.950N -100.3666). For each of the two tsunami models (SWAN and TUNAMI N2), time series of sea level were extractred from the model output at the closest model grid point to the observation location. These time series and tsunami heigts were shown in Figure 18,19 and 20. It can be seen that DART buoy (56001) and Tanahbalah tidal gauge fits well to the simulations performed using the SWAN code with GEBCO30 bathymetry. In addition, the period of the wave of tsunami appears very good at least for the first wave. Both models miss the second crest and through. Padang2 tidal gauge does not fit to the simulation performed using the SWAN code with GEBCO30 bathymetry. This could be caused by the lack of detailed nearshore bathymetry in Padang. The other reason is the water depth used in the bathymetric grid with spacing. Since the tide gaguges are usually in water less than a few meters depth, the wave amplitude at the model output point could be expected to be on average less than the observed wave amplitude at a gauge in shallower water. Nevertheless, the overall agreements are very good, especially the used fault plane and vertical dislocation models seem to yield much better results in terms of the phases. Also, the simulated maximum heights are well reproduced in DART buoy and Tanahbalah tidal gauge locations.

DISCUSSION

This study was based on the proposed fault plane models with a coupled of numerical simulations for tsunami generation and propagation in the Mentawai Island coasts. Based on the tsunami simulations, the southern part of South Pagai Island shows the earliest arrival of

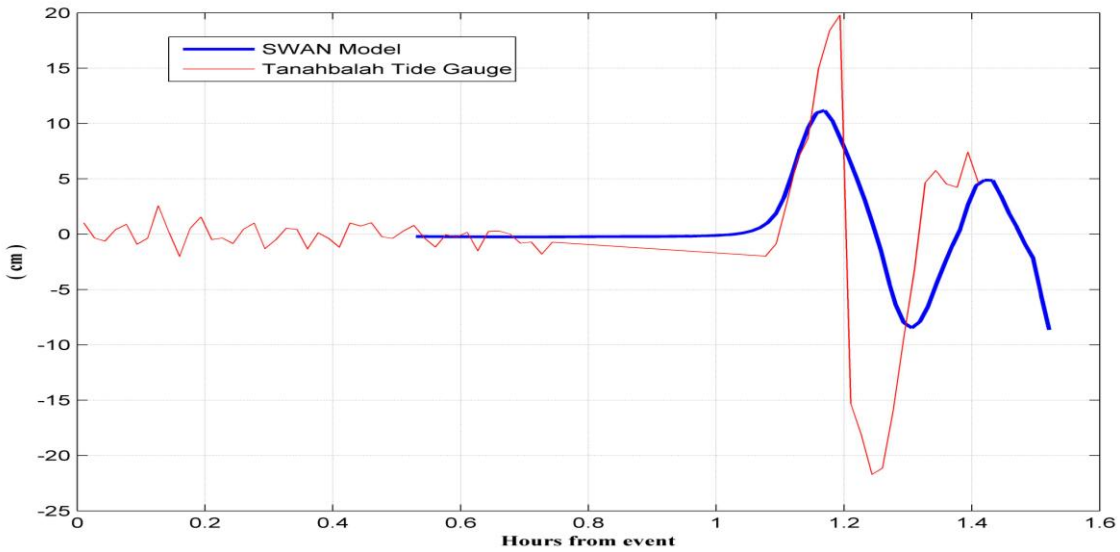

Figure 19. Comparison with Tanahbalah tide gauge measurements based on SWAN model with GEBCO30 bathymetry.

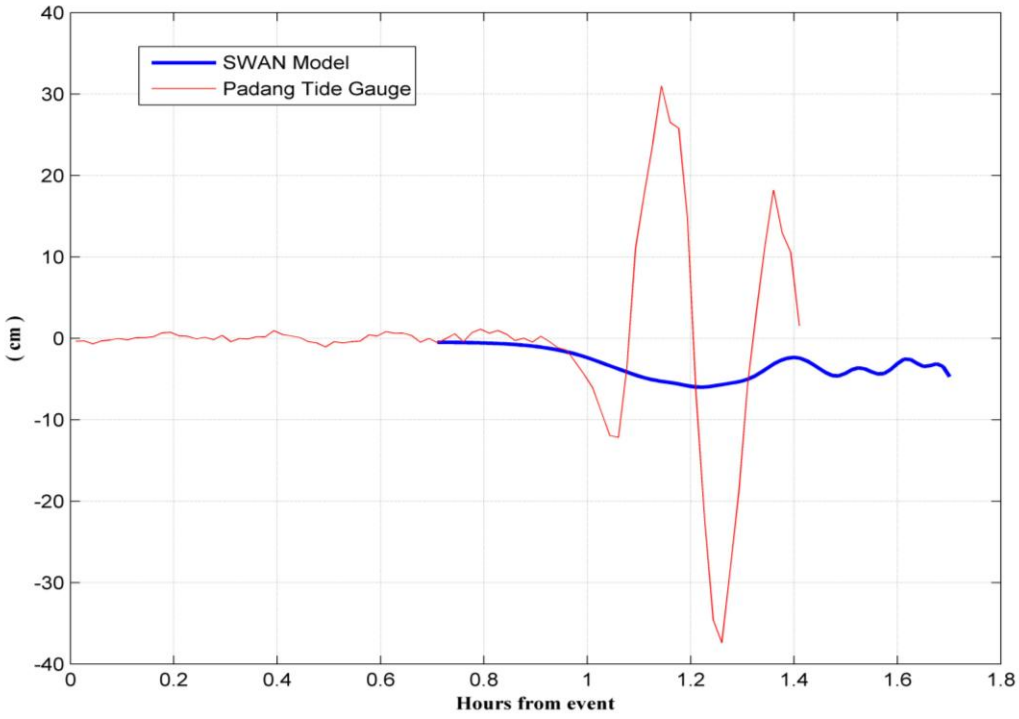

Figure 20. Comparison with Padang2 tide gauge measurements based on SWAN model with GEBCO30 bathymetry.

tsunami from the shock time which takes about 16 min to propagate.This time is not enough to evacuate and carry could affect the Mentawai Island coasts located usually no more than a hundred kilometers from the subduction out tsunami mitigation in case of a tsunami generation. However, there is always a possibility of tsunamis that zone earthquakes. Authorities for the region near the subduction zone should be aware of this possibility.

The goal of the study is not to model the inundation area of dry land, but to create a foundation for future studies that will address the maximum heights of waves for the Mentawai Island coasts. Although the results are quite preliminary, it was believed that the numerical simulation in this study has captured many of the tsunami features of the actual event. The information is critical for management decision making in the future.

In all the forecast points, it obtained a consistently smaller wave heigts than was reported on the field surveys. There could be several reosons why the smaller wave heights were consistently obtained. One reason could be that the spatial resolution of the bathymetry data may be insufficient. A second reason which may cause the amplitude difference could be the error in the rupture model. For example, if the slip was significantly over or underestimated then this could cause a change in the amplitude of the tsunami waveform.

The findings of this study could be used to prepare a pre-defined scenario database on tsunami propagation calculations for early warning systems in the region. It is believed that the findings could also be engender to calculate correct and fastly predicted tsunami wave heights in the coastal areas of Mentawai Islands. Furthermore short tsunami arrival times as it was in this study especially require a possible earthquake source parameters data on tectonic features of the faults such as strike, dip, rake and slip in order to minimize real time uncertainty of rupture parameters. Indeed the earthquake parameters available right after an earthquake are preliminary and could be inaccurate. Therefore, the findings could lead to prepare pre-defined databases, according to the seismotectonics properties of the region.

ACKNOWLEDGEMENT

The author would like to thank A. Annunziato for sharing the computer programs TAT and JRC-SWAN used for tsunami simulation and for valuable efforts to improve my studies. The long-wave propagation model, TUNAMI N2 code, used in this study, is a registered copyright of Professors F. Imamura, A.C. Yalçıner, and C.E. Synolakis. Also, sincere gratitude goes to Prof. A.C. Yalçiner and Prof. T. Taymaz for their constant encouragements and guidance over a few years back. The author would also like to express his deep appreciation to the Scientific and Technological Research Council of Turkey (TUBITAK) for the financial support throughout his post-doctoral studies in European Commission Joint Research Center related to tsunami simulation analysis.

REFERENCES

Annunziato A (2007). The Tsunamı Assesment Modellıng System by the Joint Research Center. Sci. Tsu. Hazards., 26: 70-92.

Annunziato A, Ulutaş E, Titov VV (2009). Tsunami Model Study Using JRC-SWAN and NOAA-SIFT Forecast Methods, International Symposium on Historical Earthquakes and Conservation of Monuments and Sites in the Eastern Mediterranean Region 500th Anniversary Year of the 1509. Book of Proceedings, İstanbul., pp. 131-141.

Annunziato A, Franchello G, DeGroeve T, Khudhairy DA (2010). JRC Tsunami Modelling Systems. Indian Ocean Tsunami Modelling Symposium, Fremantle, Australia, 12-15 October 2010. Book of Proceedings, pp. 9-13.

BBC 2010. No alert in Indonesian tsunami. Available from: http://www.bbc.co.uk/news/world-asia-pacific-11635714.

Borrero JC, Synolakis CE, Fritz H (2006). Northern Sumatra Field Survey after the December 2004 Great Sumatra Earthquake and Indian Ocean Tsunami. Earthquake Spectra, 22: 93-104.

ETOPO2, NGDC/NOAA: Surface of the Earth 2-minute color relief images, Available from: www.ngdc.noaa.gov/mgg/image/2minrelief.html, 2006.

Franchello G (2008). Modelling shallow water flows by a High Resolution Riemann Solver, EUR 23307 EN - 2008, ISSN 1018-5593.

GEBCO30, IHO/UNESCO:General Bathymetric Chart of the Ocean, Available from: http://www.bodc.ac.uk/data/online_delivery/gebco.

Goto C, Ogawa Y, Shuto N, Imamura F (1997). Numerical Method of Tsunami Simulation with the Leap-Frog Scheme (IUGG/IOC Time Project). IOC Manual, UNESCO, No. 35.

Goto C, Ogawa Y (1982). Numerical Method of Tsunami Simulation with the Leap-Frog Scheme, Translated for the Time Project by Shuto, N., Disaster Control Research Center, Facul. Engineer. Tohoku Univ.,

Gutscher MA, Baptista MA, Miranda JM (2006). The Gibraltar Arc seismogenic zone (part 2): Constraints on a shallow east dipping fault plane source for the 1755 Lisbon earthquake provided by tsunami modeling and seismic intensity. Tectonophysics., 426: 153–166.

Heidarzadeh M, Pirooz MD, Zaker NH, Yalçıner AC (2008). Preliminary estimation of the tsunami hazards associated with the Makran Subduction zone at the Northwestern Indian Ocean, Natural Hazards., doi:10.1007/s11069-008-9259-x.

Imamura F, Shuto N (1989). Numerical simulation of the 1960 Chilean Tsunami. In: Proceedings of the Japan–China (Taipei) Joint Seminar on Natural Hazard Mitigation, Kyoto, Japan.

Imamura F (1995). Review of tsunami simulation with a finite difference method, long-wave runup models. World Sci., pp. 25-42.

Koresawa A (2010). Field Survey of Tsunami Stricken Areas in the Mentawai Islands: focusing on policy aspects, ICA-JST Indonesia Multi-disciplinary Hazard Reduction from Earthquakes and Volcanoes in Indonesia, 5th – 10th November, Indonesia (http://www.adrc.asia/adrcreport_e/archives/2010/11/26100319.html).

Lestariningsih D (2010). Earthquake and Tsunami in Mentawai Islands by Caritas Indonesia, Availailable from: http://www.caritas.org/newsroom/press_releases/PressRelease27_10_10b.html.

Liu Y, Shi Y, Yuen DA, Sevre EOD, Yuan X, Xing HL (2009). Comparison of linear and nonlinear shallow wave water equations applied to tsunami waves over the China Sea. Acta Geotechnica, 4: 129-137.

Mader C (1988). Numerical modelling of water waves. Los Alamos series in basic and applied sciences. University of California Press, Berkeley, California, p. 206.

Okada Y (1985). Surface deformation due to shear and tensile faults in a half-space. Bull. Seism. Soc. Am., 75: 1135-1154.

Okal EA (1988). Seismic parameters controlling farfield tsunami amplitudes: A review. Nat. Hazards, 1: 67–96.

Pelinovsky E, Kharif C, Riabov I, Francius M (2001). Study of tsunami propagation in the Ligurian Sea. Nat. Hazards Earth Syst. Sci., 1: 195–201.

Shuto N, Goto C (1988). Numerical simulations of the transoceanic propagation of Tsunamis. In: Sixth Congress Asian and Pacific Regional Division, International Association for Hydraulic Research, Kyoto, Japan.

Shuto N, Goto C, Imamura F (1990). Numerical simulation as a means of warning for near-field Tsunami, Coastal Engineering in Japan. 33: 173–193.

Stein S Okal EA (2005). Size and speed of the Sumatra earthquake. Nature, 434: 581-582.

Tinti S, Armigliato A, Manucci A, Pagnoni G, Zaniboni F, Yalciner AC

Altinok Y (2006). The Generating Mechanisms Of The August 17, 1999 Izmit Bay (Turkey) Tsunami: Regional (Tectonic) And Local (Mass Instabilities) Causes. Mar. Geol., 225(1–4): 311–330.

Titov VV, Gonzales F (1997). Implementation and testing of the Method of Splitting Tsunami model, NOAA. Tech. Memo, ERL.PMEL-112: 11.

Titov VV, Synolakis CE (1998). Numerical modeling of tidal wave runup. J. Water Ports Coast Ocean Eng., 124: 157-171.

USGS 2010. Global CMT Project Moment Tensor Solution. Available from: http://earthquake.usgs.gov/earthquakes/eqinthenews/2010/usa00043nx/neic_a00043nx_gcmt.php.

Wang XM, Liu PLF (2006). An analysis of 2004 Sumatra earthquake fault plane mechanisms and Indian Ocean tsunami. J. Hydrol. Res., 44: 147-154.

Wells DL, Coppersmith KJ (1994). New empirical relationship among magnitude, rupture lenght, rupture width, rupture area, and surface displacement. Bull. Seism. Soc. Am., 84(4): 974-1002.

Yalciner AC, Synolakis AC, Alpar B, Borrero J, Altinok Y, Imamura F, Tinti S, Ersoy S, Kuran U, Pamukcu S Kanoglu U (2001). Field Surveys and Modeling 1999 Izmit Tsunami. In: International Tsunami Symposium ITS 2001, Session 4, Seattle, 7–9: 557–563.

Yalçiner A.C, Altinok Y, Synolakis CE (2000). Tsunami Waves in Izmit Bay after the Kocaeli Earthquake, Chapter 3 in the Book Earthquake Spectra. Prof. J. Earth. Eng. Res. Inst., 16: 55-62.

Yalçıner AC, Alpar B, Altinok Y, Ozbay I, Imamura F (2002). Tsunamis in the Sea of Marmara: Historical documents for the past, models for future. Mar. Geol. (Special Issue), 190: 445–463.

Yalciner A, Pelinovsky E, Talipova T, Kurkin A, Kozelkov A. Zaitsev A (2004). Tsunamis in the Black Sea: Comparison of the historical, instrumental and numerical data. J. Geophys. Res., doi:10.1029/2003JC002113, 109: C12023.

Yolsal S, Taymaz T, Yalciner AC (2008). Understanding tsunamis, potential source regions and tsunami-prone mechanisms in the Eastern Mediterranea. Geol. Soc., London, Special Publ., 291: 201-230.

Yalçıner AC, Pelinovsky E (2007). A short cut numerical method for determination of periods of free oscillations for basins with irregular geometry and bathymetry. Ocean Eng., doi:10.1016/ j.oceaneng.,2006.05.016, 34: 747–757.

Yalçıner AC, Kuran U, Akyar A, Imamura F (1995). An investigation on the generation and propagation of tsunamis in the Aegean Sea by mathematical modelling. In: Tsuchiya, Y., Shuto, N. (Eds.). Tsunami: Progress in Prediction, Disaster Prevention and Warning. Book Series of Advances in Natural and Technological Hazards Research. Kluwer. Dordrecht, pp. 55-70.

Zahibo N, Pelinovsky E, Yalciner AC, Kurkin A, Koselkov A, Zaitsev A (2003). The 1867 Virgin Island Tsunami: Observations and modelling. Oceanologica Acta, 26: 609–621.